

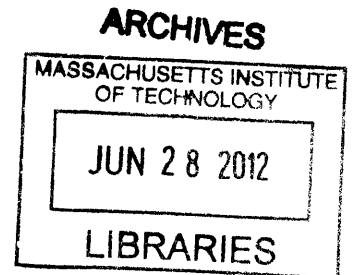
# Modeling the Chemical, Diffusional, and Thermal Processes of a Microreactor

by  
James Emanuel Silva

Submitted to the Department of Mechanical Engineering in  
Partial Fulfillment of the Requirements for the Degree of  
Bachelor of Science in Mechanical Engineering

at the  
Massachusetts Institute of Technology  
June 2012

©2012 Massachusetts Institute of Technology  
All rights reserved



Signature of Author: .....

A handwritten signature in black ink, appearing to be "James Emanuel Silva", written over a horizontal dotted line.

Department of Mechanical Engineering  
May 29, 2012

Certified by: .....

A handwritten signature in black ink, appearing to be "Evelyn N. Wang", written over a horizontal dotted line.  
Evelyn N. Wang  
Assistant Professor of Mechanical Engineering  
Thesis Supervisor

Accepted by: .....

A large, handwritten signature in black ink, appearing to be "John H. Lienhard V", written over a horizontal dotted line.  
John H. Lienhard V  
Samuel C. Collins Professor of Mechanical Engineering  
Undergraduate Officer



# Modeling the Chemical, Diffusional, and Thermal Processes of a Microreactor

by

James Emanuel Silva

Submitted to the Department of Mechanical Engineering on May 29<sup>th</sup>, 2012, in Partial Fulfillment of the Requirements for the Degree of Bachelors of Science in Mechanical Engineering

## Abstract

This thesis seeks to create a high fidelity model of the multiphysics present in a typical microreactor using propane combustion as a fuel source. The system is fully described by energy, momentum, and mass equations, all of which are highly coupled by their dependence on temperature. Using the work done on the S $\mu$ RE IV microreactor as a basis, this undergraduate thesis implements the relevant equations of a general microreactor model in the finite element software known as COMSOL Multiphysics. Combustion was modeled as a surface reaction occurring on the microchannel walls, with rates modeled based on Arrhenius assumptions. Furthermore, a compressible Navier-Stokes equation was applied to describe the gas flow. Finally, Maxwell-Stefan equations were implemented in order to capture the concentration and temperature dependence of the various species diffusivities. For characterizing the thermal profile, convective, conductive, and radiative heat transfer modes were all included. However, because this ideal model faced convergence issues due to the complexity of the Maxwell-Stefan diffusion equations, a simpler model is presented. The simpler model assumed general convective and conductive mass transfer, with diffusivity values typical of gas-gas mass transfer utilized. Furthermore, the flow was also simplified to be described by the incompressible Navier-Stokes equation. Temperatures from this simplified simulation ranged from 850-856K as compared to previous results, which showed a range of approximately 850-920K. Furthermore, propane concentration only fell from 0.150 mol m<sup>-3</sup> to 0.100 mol m<sup>-3</sup> while previous results showed complete consumption for the same initial amount. These differences were anticipated and are thereby explained by the simplifications made. Finally, several steps are outlined for future investigation as to the problems facing the ideal model. These steps include analysis not only of the equations implemented by COMSOL, but also of numerical factors that could hinder convergence. Fixing the ideal model should allow for application to various projects that would require chemical or thermal data of such a microreactor.

Thesis Supervisor: Evelyn N. Wang

Title: Assistant Professor, Mechanical Engineering



# Acknowledgements

This thesis would not have been made possible without the key contributions of several individuals. Though some of them may not see this thesis, I hope they all know how much I have appreciated their support.

First and foremost, I would like to thank my advisor, Professor Evelyn Wang. Her insightfulness saved me several hours of wasted effort on a few occasions, and her guidance helped me to see hope amongst errors. In particular, I really appreciate the fact that Professor Wang's concerns extended beyond my thesis work and to other aspects of my life. If there were more professors like Professor Wang, I think many more students would opt to pursue PhDs.

Additionally, Professor Youngsuk Nam invested an incredible amount of time teaching me what it means to be a research scientist. His attention to detail and his high expectations helped push me to really embrace this research project and make it my own. Even when out of the country, Professor Nam made time to meet on a weekly basis, making me feel that I was still a priority despite his many commitments. As I leave MIT, I am very proud to have Professor Nam as a colleague, and I hope that he feels the same way.

I admire Kevin Bagnall for continually opting to sit at his desk in the RK Lab, knowing that I could come in any minute and bug him with questions. Kevin saved me a lot of time not only by helping to familiarize me with the lab, but also for just being a general go-to guy.

Finally, I would like to thank my mother and father, Albertina and Joe Silva, for putting up with the stress I went through at times. They had the good judgment to know when (and when not) to ask about my thesis progress.



# Table of Contents

|                                  |    |
|----------------------------------|----|
| Chapter 1: Introduction          | 11 |
| 1.1: Simulation.....             | 11 |
| 1.2 COMSOL.....                  | 12 |
| 1.3 Microreactor.....            | 12 |
| 1.4 Thesis Objective.....        | 13 |
| <br>                             |    |
| Chapter 2: S $\mu$ RE IV         | 14 |
| 2.1: Geometry .....              | 14 |
| <br>                             |    |
| Chapter 3: Model                 | 16 |
| 3.1: Simulation Geometry.....    | 16 |
| 3.2: Governing Equations .....   | 17 |
| 3.3: Chemical Parameters .....   | 20 |
| 3.4 Thermal Parameters .....     | 21 |
| 3.5: Implemented Conditions..... | 21 |
| 3.6: Assumptions.....            | 22 |
| 3.7: Boundary Conditions .....   | 23 |
| <br>                             |    |
| Chapter 4: Results               | 25 |
| 4.1: Analysis .....              | 25 |
| 4.2: Conclusions.....            | 29 |
| 4.3: Future Work.....            | 31 |
| <br>                             |    |
| Appendix A: Parameter List       | 33 |
| <br>                             |    |
| Bibliography                     | 34 |





# List of Figures

Figure 1. Schematic of the process for etching the high temperature reaction zone of S $\mu$ RE IV[5].  
A serpentine pattern of several turns was chosen in order to allow combustion to go to completion. Though the initial wafer was 150mm thick, the final product was just 1.3mm thick..... 14

Figure 2. Final assembly of S $\mu$ RE IV [5]. The glass capillaries extend out from the inlet and outlet, allowing the gaseous mixture to flow through the microreactor. .... 15

Figure 3. Microchannel geometry used for simulation. The highlighted region in pink indicates the channel for gas flow, while the surrounding material is silicon of the microreactor..... 16

Figure 4. As expected, the reaction rate is very high initially, but quickly decays as products are consumed. Though the numbers shown are lower than would be expected, the pattern is consistent..... 25

Figure 5. Propane concentration profiles for a) 1m/s and b) 0.3m/s. Here, the higher flow rate contributes to the further dispersion of propane. .... 27

Figure 6. Stead-state propane concentration profile for flow rates of (a) 6sccm, (b) 8 sccm, and (c) 10 sccm [5]. .... 27

Figure 7. Cross-sectional plot of temperature within flow and surrounding silicon. .... 28

Figure 8. Comparison of (a) experimental temperature profile to (b) simulated temperature profile for the combustion of 6 sccm of propane in a 16 mTorr vacuum. .... 29



# Chapter 1: Introduction

## 1.1: Simulation

As computers become faster and more powerful, the importance of simulation continues to grow [1]. Simulation has proven to be an important tool for researchers of all disciplines, often saving considerable time and money that would normally be spent on the construction of real life test models. However, perhaps the most important benefit of simulation is in the flexibility it allows for exploring design modifications. Once the appropriate time and effort have been invested in creating the system model, it often just takes a few clicks of the mouse to generate new analysis under a different set of parameters. In particular, this has important implications for the process of optimization, as it allows one to take a “brute force” method of finding a local optimization over a given range of supplied parameters. While such an approach may be somewhat costly in terms of the time required to compute the solutions, it is often the best course of action for problems in which several parameters are highly coupled. For these problems, design tradeoffs are not linear, making it difficult to envision an optimized system.

With that being said, simulation should not be taken as a miracle approach capable of solving all of one’s problems. There is a certain art to the process, though this idea may have been drowned out by the overwhelming number of too complex models. Above all, it is paramount to create the simplest model that is still representative of the system. Too often individuals become obsessed with modeling every detail imaginable, creating system models that are far too complex to be properly simulated. In order to be successful with this process, one must understand what details are and are not vital to properly representing their system. Understanding the importance and optimization of a few key parameters is more meaningful than going about the same task with one or two dozen variables.

While the concept of simulation brings to mind a high-level process of choosing parameters and model specifications, finite element analysis is what really what makes the entire concept possible. The highly coupled nature of many of the problems solved via simulation is due to the fact that the governing equations are partial equations. Not surprisingly, the challenge in solving these partial differential equations is in generating solutions that reflect the system and

simultaneously remain numerically stable for variations in inputs. Whereas twenty years ago, the process of creating a solver capable of generating such solutions would have easily generated a PhD thesis, today there are many numerical packages available commercially. In particular, this undergraduate thesis uses one known as COMSOL Multiphysics.

## **1.2 COMSOL**

COMSOL Multiphysics is a finite element analysis, simulation package, and solver available on the commercial market. The software contains packages for various engineering and physics applications (called modules) and takes its name “multiphysics” from the ease in which these various applications can be coupled to reflect real world problems. One of COMSOL’s key features is an extensive MATLAB interface that allows MATLAB functions to be used for defining system parameters in simulations. Additionally, simulation results from COMSOL can also be exported to a MATLAB environment to allow for more complicated post-processing.

In particular, this work uses COMSOL 3.5a. For this version, a separate (but related) product was released by COMSOL, known as the COMSOL Reaction Engineering Lab. This software allows users to define chemical equations that model reacting systems. It solves material and energy balances for such systems, but is limited to cases in which composition and temperature vary only with time. For space-dependent models, the Reaction Engineering Lab features a direct export to models in the Chemical Engineering Module with COMSOL Multiphysics. These models include expressions for reaction kinetics that were defined in the Reaction Engineering Lab. Once relevant properties have been exported to the Chemical Engineering Module, various other modules (such as heat transfer and diffusion modules) can also be defined and coupled to the space-dependent reaction kinetics.

## **1.3 Microreactor**

This undergraduate thesis focuses on the thermal characterization of a microreactor. By definition, a microreactor is a miniature housing for carrying out chemical reactions. Microreactors perform three basic functions: initiating and facilitating reaction through mixing

of the reactants, providing time and volume to allow the reaction to go to completion, and providing/removing heat.

Given their design, microreactors pose several advantages over traditional batch reactors. Their high surface-to-volume ratio allows for accelerated reaction rates when compared to macroscopic devices, while high heat and mass transfer rates allow for high yields of chemical products. The applications of such technology range from the pharmaceutical industry [2] to bio-engineering [3], and the application in thermophotovoltaic (TPV) technology in particularly intriguing [4]. Chapter 2 discusses the geometry of S $\mu$ RE IV [5], a particular microreactor geometry that provided a general basis of study for this thesis.

## **1.4 Thesis Objective**

The goal of this thesis is twofold. First, this thesis seeks to create a high fidelity model of a typical microreactor setup. In order to do this, the proper chemical, diffusional, and thermal processes needed to be adequately modeled, especially with regards to their coupling. If successful, such a model would be applicable to design considerations for many different applications. Second, this thesis also serves as an exploration for COMSOL's ability to capture chemical kinetics and incorporate them in a modeling environment. Such information is applicable to several projects currently taking place in the Rohsenow Kendall Heat and Mass Transfer Laboratory and will be conveyed to appropriate projects.

## Chapter 2: S $\mu$ RE IV

### 2.1: Geometry

S $\mu$ RE IV is a microreactor designed by Blackwell with the objective of supporting high temperature (800°C) chemical combustion. The microchannels were manufactured through the wet KOH etching of 150mm thick silicon wafers. The channel height measured 750 $\mu$ m while the width measured 500 $\mu$ m.

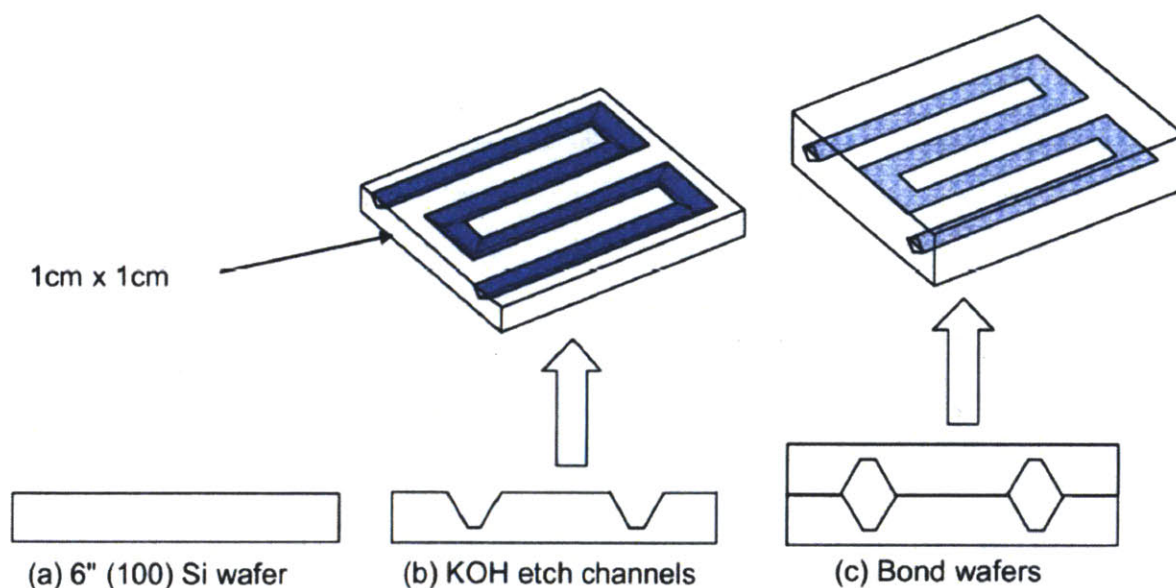


**Figure 1. Schematic of the process for etching the high temperature reaction zone of S $\mu$ RE IV[5]. A serpentine pattern of several turns was chosen in order to allow combustion to go to completion. Though the initial wafer was 150mm thick, the final product was just 1.3mm thick.**

Evenly distributed amongst the four walls of the microchannel was a catalyst, 5wt% Pt on  $\gamma$ -Al $_2$ O $_3$ . In this setup, it was assumed that the propane/oxygen mixture was perfectly mixed and did not begin reacting until reaching the inlet (and coming into contact with the catalyst). The combustion of propane is described by Equation 1:



Relevant equations regarding the modeling of the reaction rate, heat of reaction, and various parameters are described in Chapter 3.



**Figure 2. Final assembly of S $\mu$ RE IV [5]. The glass capillaries extend out from the inlet and outlet, allowing the gaseous mixture to flow through the microreactor.**

# Chapter 3: Model

## 3.1: Simulation Geometry

Due to time constraints, a precise model of S $\mu$ RE IV was not created. Instead, a 15mm long microchannel with surrounding silicon was created. This channel maintained the dimensions of S $\mu$ RE IV (500 $\mu$ m width and 750 $\mu$ m height), but did not include the serpentine pattern. For analyzing heat transfer to the silicon, an additional width of 500 $\mu$ m and an additional height of 750 $\mu$ m were added for the silicon enclosure.

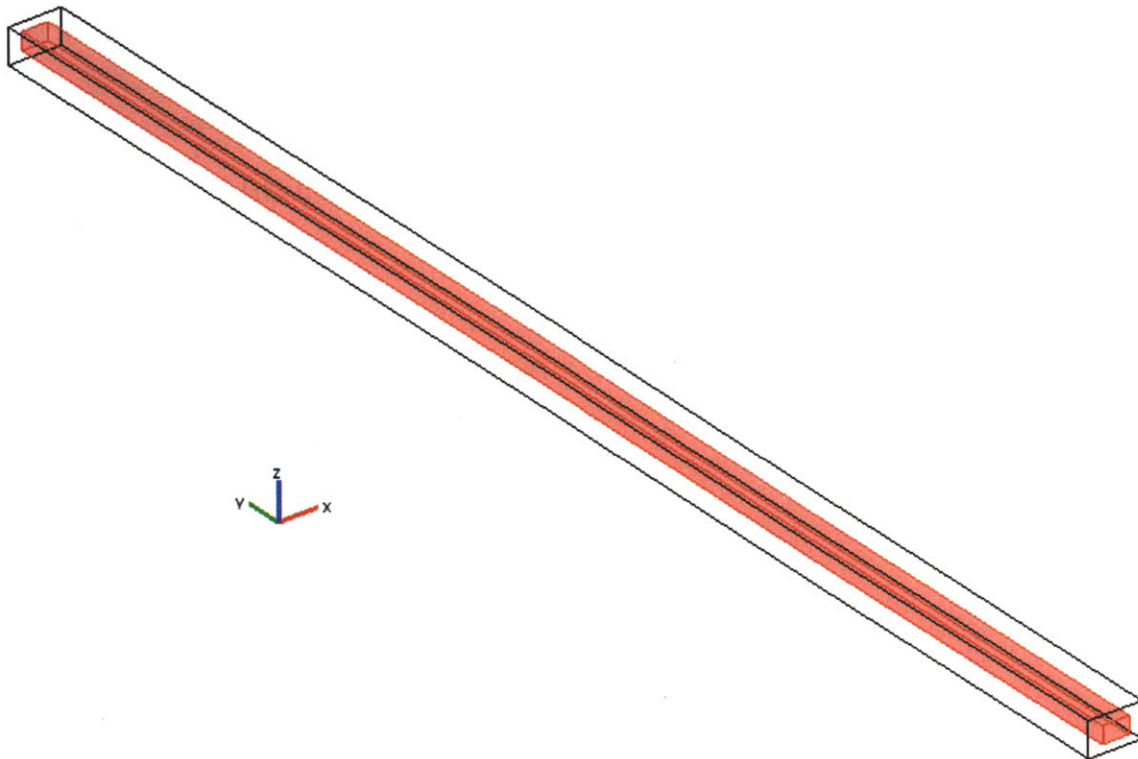


**Figure 3. Microchannel geometry used for simulation. The highlighted region in pink indicates the channel for gas flow, while the surrounding material is silicon of the microreactor.**



## 3.2: Governing Equations

The model developed in COMSOL uses a finite element method to simultaneously solve for the flow field, thermal profile, and individual species concentrations. The multiphysics problem becomes quite complicated, as each equation shows some temperature dependence.

Beginning with the conservation of mass yields the following equation:

$$\nabla \cdot (\rho \mathbf{u}) = 0 \quad (2)$$

In Equation 2,  $\rho$  is the density of the gas mixture while  $\mathbf{u}$  is the 3D vector of the mass-averaged velocity. In this system, it is important to note that the density can change in two ways. First, the consumption of reactants and generation of products changes the mole fraction of each species, thereby changing the mixture density. Second, variations in temperature also contribute to the expansion and contraction of the gas mixture.

To account for these variations in mixture density, it is assumed that the gas mixture is composed of gases obeying the ideal gas law. Because the operating pressure is much less than the critical pressure of the system, and because the Mach number is always much less than 1, these assumptions are valid. Thus, the density of the multi-component gas mixture can be written as:

$$\rho = \frac{P_0}{TR_g} \sum_i x_i M_i \quad (3)$$

In Equation 3,  $P_0$  is the operating pressure,  $T$  is the temperature,  $R_g$  is the universal gas coefficient, and  $x_i$  and  $M_i$  are the molar fractions and molecular weights of species  $i$ .

Given the dimensions of the microreactor and the fact that the flow velocity ranges between 0.1m/s and 5m/s, it is safe to assume that the gas flow is always laminar. This allows application of what COMSOL denotes as the equation for general laminar flow:

$$\rho(\mathbf{u} \cdot \nabla \mathbf{u}) = \nabla \cdot \left[ -p\mathbf{I} + \eta(\nabla \mathbf{u} + (\nabla \mathbf{u})^T) - \left( \frac{2\eta}{3} - \kappa_{\text{div}} \right) (\nabla \mathbf{u})\mathbf{I} \right] + \mathbf{F} \quad (4)$$

In Equation 4,  $p$  is the pressure of the mixture,  $\eta$  is the dynamic viscosity,  $\kappa_{\text{div}}$  is the dilatational viscosity, and  $\mathbf{F}$  is an external force vector.

With regards to energy balance, this model takes into account convection and conduction as primary modes of heat transfer within the silicon of the microreactor. This equation is given by:

$$\nabla \cdot (-k\nabla T) = Q - \rho C_p \mathbf{u} \cdot \nabla T \quad (5)$$

Here,  $k$  is the thermal conductivity of silicon,  $Q$  is the external heat, and  $C_p$  is the heat capacity of silicon at constant pressure.

In the case of the flow, it is important to capture the effects of species diffusion on the energy balance equation. Letting  $\nabla H_{p,i}$  be the partial molar enthalpy of species  $i$  and  $N_{D,i}$  the molecular molar flux of species  $i$  with respect to mass averaging, Equation 5 becomes:

$$\nabla \cdot (-k\nabla T) = Q - \rho C_p \mathbf{u} \cdot \nabla T + \sum_i (\nabla H_{p,i} \cdot N_{D,i}) \quad (6)$$

As mentioned before, COMSOL uses a module known as Maxwell-Stefan Diffusion for modeling concentration dependent diffusion. In this module, it is necessary to construct the Maxwell-Stefan diffusivity matrix, a matrix composed of the multicomponent Fick diffusivities. The governing equation of this module is given by:

$$\frac{\partial}{\partial t} (\rho \omega_i) + \nabla \cdot (\mathbf{j}_i + \rho \omega_i \mathbf{u}) = R_i \quad (7)$$

Rather than work with mole fractions, the Maxwell-Stefan module solves for the mass fraction ( $\omega_i$ ) of species  $i$ .  $R_i$  is the reaction rate for species  $i$  of the combustion process outlined in Equation 1, while  $\mathbf{j}_i$  describes the diffusion-driven transport, as outlined by Curtiss [6] and Bird [7]. This transport is a function of temperature and a diffusional driving force  $\mathbf{d}_j$ :

$$\mathbf{j}_i = (-D_i^T \nabla \ln T) - \rho_i \sum_{j=1}^n \bar{D}_{ij} \mathbf{d}_j \quad (8)$$

Here,  $D_i^T$  denotes the generalized thermal diffusion coefficient while  $\bar{D}_{ij}$  is the  $ij$  component of the multicomponent Fick diffusivity. In Equation 8,  $\mathbf{d}_j$  accounts for diffusional driving forces through concentration, pressure and external forces. Substituting Equation 8 into Equation 7 gives the mass transport equation set up by the application mode:

$$\frac{\partial \rho \omega_i}{\partial t} + \nabla \cdot \left( \rho \omega_i \mathbf{u} - \rho \omega_i \sum_{j=1}^n \bar{D}_{ij} \left( \nabla x_j + (x_j - \omega_j) \frac{\nabla p}{p} \right) - D_i^T \frac{\nabla T}{T} \right) = R_i \quad (9)$$

To solve Equation 9, it is necessary to specify the multicomponent Fick diffusivities. For four components or more, the multicomponent Fick diffusivities are obtained numerically through matrix inversion. COMSOL Multiphysics starts with the multicomponent Maxwell-Stefan diffusivity matrix  $D$  to compute the multicomponent Fick diffusivity matrix ( $\bar{D}$ ) using the equation

$$\bar{D}_{ij} = N_{ij} - g \quad (10)$$

where  $ij$  are indices in the matrices  $\bar{D}$  and  $N$  range from 1 to the number of components,  $n$ . The elements of the matrix  $N$  in Equation 10 are defined as

$$N_{ij} = (P^{-1})_{ij} \quad (11)$$

where  $P^{-1}$  is the inverse of a matrix  $P$ . The matrix  $P$  is defined as

$$P_{ij} = \frac{\omega_i \omega_j}{g} - C_{ij} \quad (12)$$

where the matrix  $\bar{C}$  is defined as:

$$\bar{C}_{ij} = \begin{cases} \frac{x_i x_j}{D_{ij}} & i \neq j \\ -\sum_{k \neq j} \bar{C}_{ik} & i = j \end{cases} \quad (13)$$

The term  $g$  in Equation 12 is a scalar value that provides numerical stability and should be of the same order of magnitude as the multicomponent Maxwell-Stefan diffusion coefficients. The application mode therefore defines  $g$  as the sum of the multicomponent Maxwell-Stefan diffusion coefficients:

$$g = \sum_{i=1}^{n-1} \left( \sum_{j=i+1}^n D_{ij} \right) \quad (14)$$

For low-density gas mixtures, the multicomponent Maxwell-Stefan diffusivities,  $D_{ij}$ , can be replaced with the binary diffusivities for all pairs of species.

### 3.3: Chemical Parameters

The chemical reaction from Equation 1 was modeled with a forward reaction rate constant  $k_{rate}$  given by the Arrhenius expression:

$$k_{rate} = Ae^{E_a/RT} \quad (15)$$

Here,  $E_a$  is the activation energy,  $A$  is the pre-exponential factor,  $R$  is the universal gas constant, and  $T$  is the temperature. Completing the Arrhenius expression and solving for the reaction rate  $R$ :

$$R = k_{rate}[C_3H_8][O_2]^5 \quad (16)$$

Finally, it is necessary to solve for the heat source of reaction,  $Q_{react}$ . By definition, this quantity is defined to be  $Q_{react} = -HR$ , where  $R$  is defined as above and  $H$  is the enthalpy of reaction given by:

$$H = -h_{C_3H_8} - 5h_{O_2} + 4h_{H_2O} + 3h_{CO_2} \quad (17)$$

An equation approximating  $h_i$  is given by Gordon and McBride [8] in the following form:

$$h_i = R_g \left( a_1 T + \frac{a_2}{2} T^2 + \frac{a_3}{3} T^3 + \frac{a_4}{4} T^4 + \frac{a_5}{5} T^5 + a_6 \right) \quad (18)$$

The constants  $a_1$  through  $a_6$  are numerical fits typically recorded in the CHEMKIN format [9].

### 3.4 Thermal Parameters

Through the application of effective medium theory, it is possible to calculate the macroscopic properties of the evolving gas mixture. For instance, letting  $i$  be one of the constituent species, the thermal conductivity can be defined as [10]:

$$k = 0.5 \left( \sum_i x_i k_i + \left( \sum_i \frac{x_i}{k_i} \right)^{-1} \right) \quad (19)$$

Likewise, heat capacity at constant pressure can be taken as:

$$c_p = \sum_i w_i \frac{C_{p,i}}{M_i} \quad (20)$$

### 3.5: Implemented Conditions

Due to various complications resulting from time and issues with convergence, the full model outlined above faced several convergence issues. Thus, in order to verify the design methodology, simpler models for diffusion and fluid flow were implemented.

Rather than use the Maxwell-Stefan Diffusion module to account for the concentration and temperature dependent diffusivities, a general convection and conduction application was used. While this module is better suited for mixtures in which the properties of a solvent are dominant,

its successful implementation offers some insight as to the limitations due to diffusion. For this module, the governing application was given by:

$$\frac{\partial c_i}{\partial t} + \nabla \cdot (-D_i \nabla c_i) = R_i - \mathbf{u} \nabla c_i \quad (21)$$

For a given species  $i$ ,  $c_i$  is the concentration,  $D_i$  denotes the diffusion coefficient,  $R_i$  is the reaction rate, and  $\mathbf{u}$  is the velocity vector. Representative values of  $\sim 10^{-5}$  m<sup>2</sup>/s were used for the various gas diffusivities. Furthermore, the reaction was modeled to occur in the flow itself, as opposed to occurring as surface reactions on the channel walls.

Likewise, due to similar issues facing the equations for the General Laminar Flow module, the incompressible Navier-Stokes equation was also implemented. Though this module fails to capture the variation in mixture density, it did allow the simulation to properly converge. Here, the equation for  $p$  and  $\mathbf{u}$  is given by:

$$\rho \frac{\partial \mathbf{u}}{\partial t} + \rho (\mathbf{u} \cdot \nabla) \mathbf{u} = \nabla \cdot [-p\mathbf{I} + \eta(\nabla \mathbf{u} + (\nabla \mathbf{u})^T)] + \mathbf{F} \quad (22)$$

### 3.6: Assumptions

In order to simplify the model, it was necessary to make several assumptions. As noted before, given the operating pressure of 1atm and the relatively low speeds of gas flow, the gaseous mixture was assumed to obey the ideal gas law. Furthermore, given a maximum Reynolds number of roughly 1000, the assumption of laminar flow remained valid in all cases.

Additionally, gravitational effects were neglected. The small length scale of the channel, combined with the low density of the gas mixture ( $\sim 0.10$  kg/m<sup>3</sup>) made this a fair assumption as well.

The chemical reactions taking place were all modeled as surface reactions on each of the microchannel walls. Given that the thickness of the catalyst layer ( $\sim 50\mu\text{m}$ ) was considered negligible, diffusion across it was not considered. With regards to the chemical reaction, a simple, one step mechanism for propane consumption was used. Additionally, the reaction rate was assumed to follow Arrhenius type behavior.

### 3.7: Boundary Conditions

Because the setup was assumed to be in a vacuum, convective heat transfer occurring at the external boundaries could be taken as zero. However, given the high temperatures the microreactor was expected to reach (800-1000K), radiative heat transfer could not be ignored. Thus, radiative flux boundary conditions were imposed on all external walls, with the emissivity of silicon taken to be 0.65 and the ambient temperature set to 300K.

When modeling the thermal boundary condition at the flow inlet, there was some difficulty in choosing a condition that properly captured the physics at play. Initially it was thought that an insulated boundary condition would be appropriate in order to allow only the heat of reaction to influence the local temperature profile. Unfortunately, attempts to work with this condition were met with convergence issues. Analyzing the unconverged solution that resulted from this choice of boundary condition seemed to suggest that the model was not well formed, as temperatures at the inlet boundary could not be calculated.

The next thought was to set a convective flux condition at the inlet. This boundary condition assumes that all energy passing through a specified boundary does so through the convective flux mechanism. This firstly assumes that any heat flux due to conduction across the boundary is zero

$$\mathbf{q}_{\text{cond}} \cdot \mathbf{n} = -k\nabla T \cdot \mathbf{n} = 0 \quad (23)$$

which in turn implies that

$$\mathbf{q} \cdot \mathbf{n} = \rho C_p T \mathbf{u} \cdot \mathbf{n} \quad (24)$$

This condition also seemed reasonable, given the low thermal conductivity ( $\sim 0.1 \text{ W m}^{-1} \text{ K}^{-1}$ ) and the velocity of the gas mixture. However, this boundary condition also created convergence issues. As a result, a fixed temperature of 850K was prescribed to the inlet condition. This condition was not desirable, as it acts as an effective heat sink and has considerable impact on local temperature. Since it was the only condition that would allow the simulation to converge, simulation proceeded with this condition.

For the diffusion module, fixed concentrations were applied at the inlet:  $0.15 \text{ mol m}^{-3}$  for propane,  $0.70 \text{ mol m}^{-3}$  for oxygen,  $0 \text{ mol m}^{-3}$  for  $\text{H}_2\text{O}$ , and  $0 \text{ mol m}^{-3}$  for carbon dioxide.

Diffusion was only considered in the channel, and was therefore prevented from occurring through the channel and into the silicon. With regards to the outlet, a convective flux condition was set. This convective flux is the mass transfer analogy of Equation 21:

$$\mathbf{n} \cdot (-D_i \nabla c_i) = 0 \quad (25)$$

Finally, for the momentum module, an inlet velocity of 0.3m/s was specified, with an outlet pressure of 1atm. No-slip conditions were applied to the channel walls.



# Chapter 4: Results

## 4.1: Analysis

Presented here is the data produced by the simplified model. As shown by the cross-sectional plot in Figure 4, the reaction rate is very high close to the inlet and gradually decays down the length of the channel. Coming into contact with the catalyst, the reaction initially begins with a high reaction rate, but begins slowing down as more and more of the reactants (propane and oxygen) are consumed. This is consistent with the propane concentration profile shown in Figure 5 and with Equation 16, which shows how the reaction rate scales with these quantities.

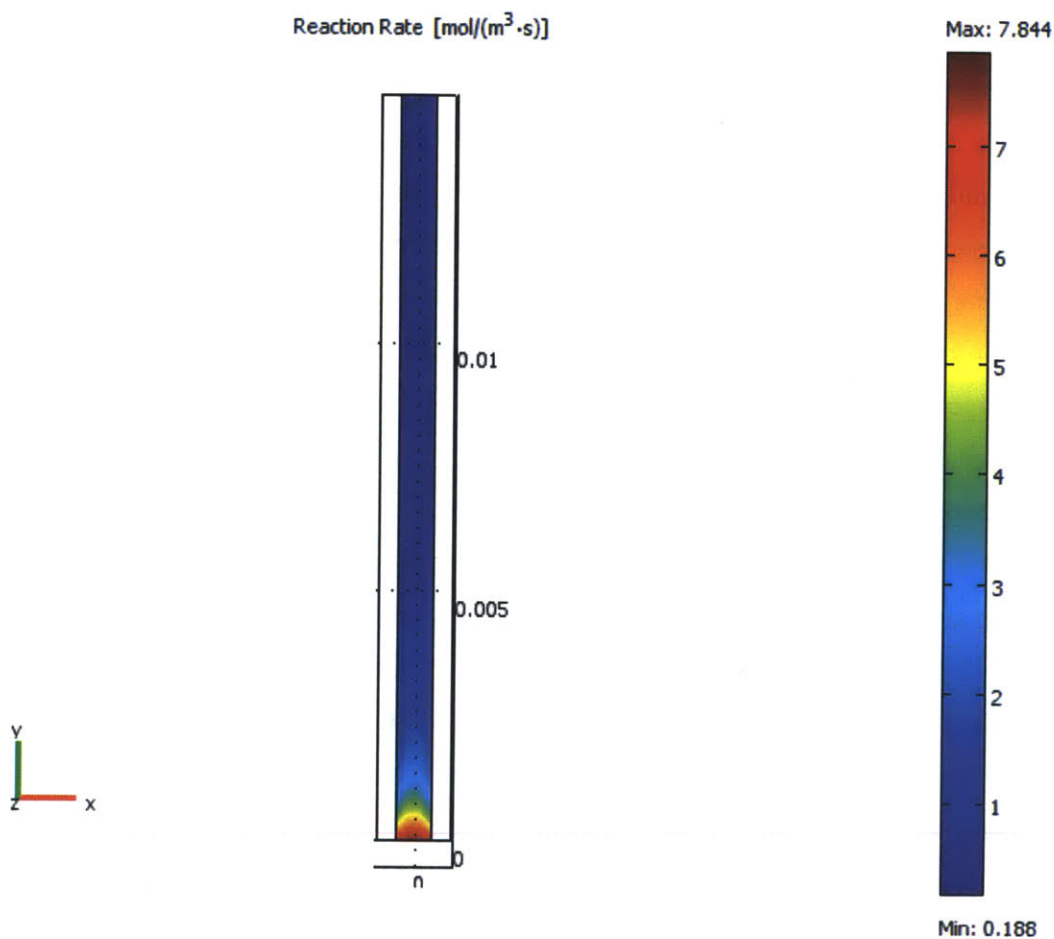


Figure 4. As expected, the reaction rate is very high initially, but quickly decays as products are consumed. Though the numbers shown are lower than would be expected, the pattern is consistent.

As expected, this simulation data is not in perfect agreement with the experimental data given the simplifications made to the model. For combustion of propane at 800°C, a reaction rate of 930 moles m<sup>-3</sup> s<sup>-1</sup> was recorded [5], two orders of magnitude beyond what this simulation observed. This disparity, however, can be explained in terms of the simplifications made to the model. For instance, by imposing the fixed temperature condition on the inlet, the local temperature profile would have been affected in the way described in Section 3.7, in turn affecting the temperature dependence of the reaction rate. Another possible explanation could be due to ambiguity in defining the pre-exponential factor in Equation 15. With Blackwell never stating the value used for his simulations, literature searches failed to deliver consistent results compatible with the experimental setup. As a result, a best guess value was chosen. Finally, it is also worth noting that Blackwell used gas flow rates that were roughly one order of magnitude beyond those in this thesis model. This fact has a direct impact on the reaction rate, and thereby also helps to greatly (but not completely) account for the difference as well.

Figure 5 shows the effect that the reaction rate has on propane concentration. With the diminishing reaction rate eventually reaching a constant value, the propane concentration behaves similarly along the channel length. Again, another expectation with the implemented reaction kinetics was that this reaction would not go to completion in the length scale provided. By assigning constant diffusivities in the simplified model, the effects of temperature and concentration on diffusivity were not captured. As a result, the constant values at times undershot the true values, especially in the hotter areas closer to the inlet. All in all, it can be seen that the implemented reaction chemistry does a reasonable job of capturing the general picture of the combustion process given the limits of the simplified model. By fixing the full model, it is expected that the results in Figure 5 will look more like Blackwell's model in Figure 6, generally showing greater length scales associated with great consumption of propane.

Comparing Figures 5 and 6, one point that becomes very apparent is the difference that flow velocity plays on species diffusion. Results from COMSOL show that for an increase in flow velocity, reaction rate decrease. As Figure 5 seems to indicate, a faster flow seems to lower the reaction rate by reducing the effective amount of propane that can take place in the reaction. However, Blackwell's results indicate the opposite. For faster flow rates, more and more of the propane seems to react near the inlet. Even though the reactions in this model were modeled as occurring in the flow while Blackwell's were modeled as surface reactions, this should not

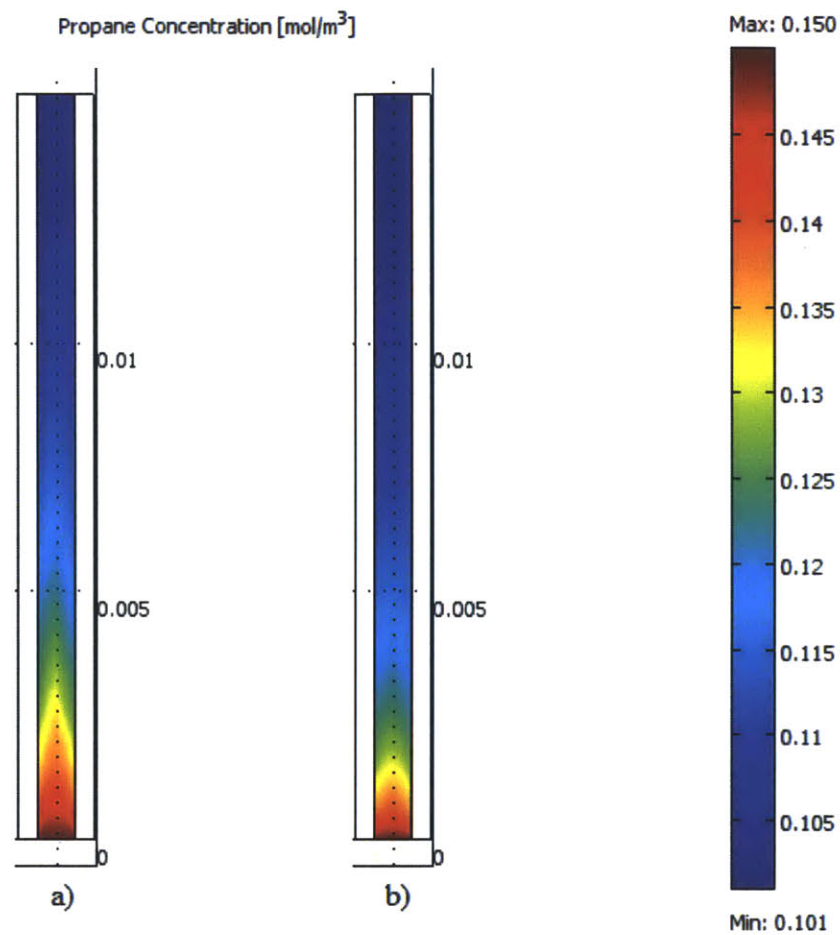


Figure 5. Propane concentration profiles for a) 1m/s and b) 0.3m/s. Here, the higher flow rate contributes to the further dispersion of propane.

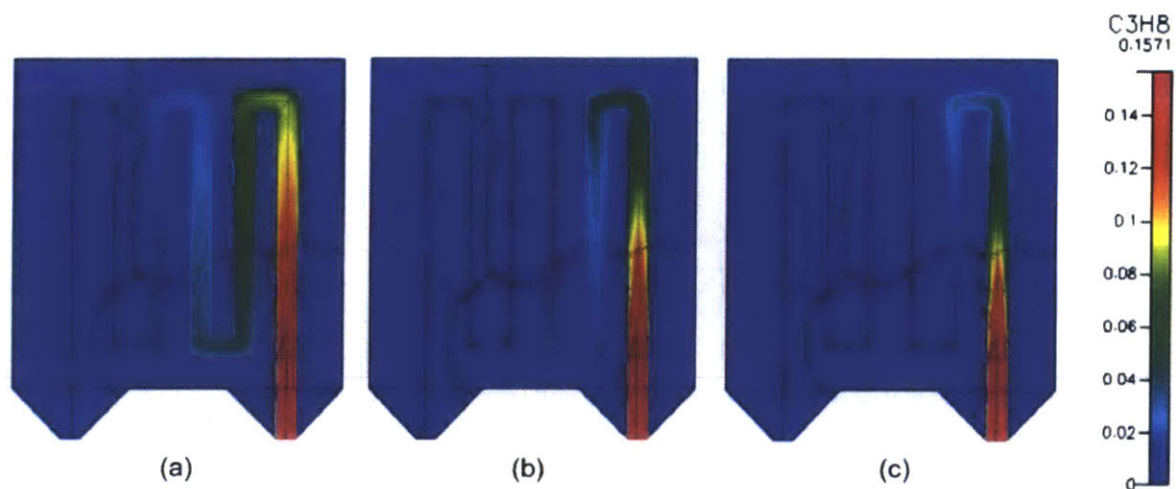


Figure 6. Stead-state propane concentration profile for flow rates of (a) 6sccm, (b) 8 sccm, and (c) 10 sccm [5].

account for the discrepancy. This is one point that particularly requires fuller investigation as the simplifications made for the modified model do not account for the behavior.

Finally, Figures 7 and 8 present the temperature profile throughout the channel and surrounding silicon. In Figure 7, the initial flare up due to combustion at the inlet is marked by a sudden spike in temperature, as noted by Blackwell. Again, consistent with the reaction rate profile, this temperature spike occurs closer to the inlet than expected.

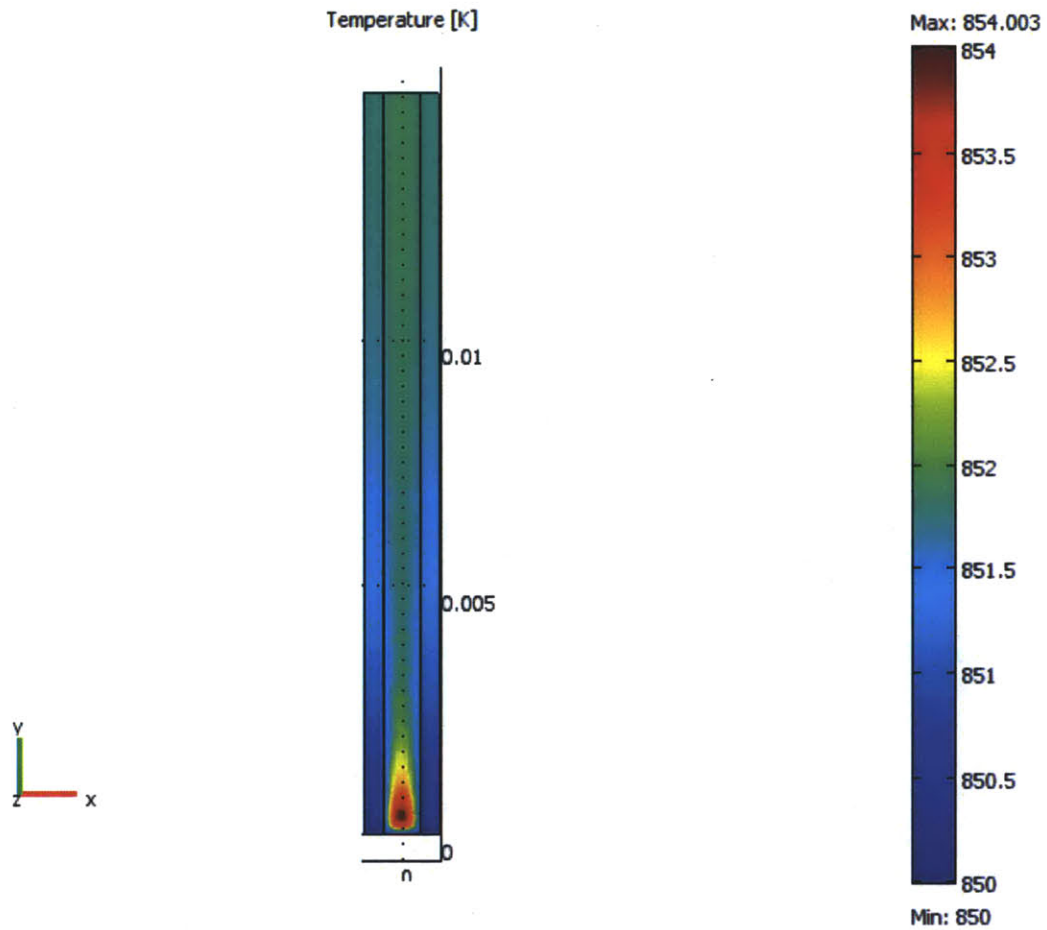
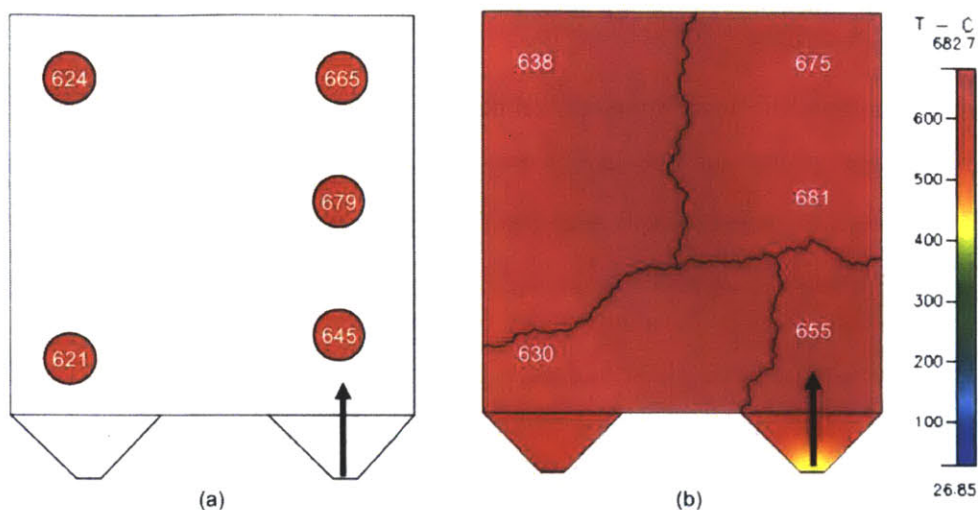


Figure 7. Cross-sectional plot of temperature within flow and surrounding silicon.



**Figure 8. Comparison of (a) experimental temperature profile to (b) simulated temperature profile for the combustion of 6 sccm of propane in a 16 mTorr vacuum.**

Also worth noting in Figure 7 is the large temperature gradient between the gaseous flow and the silicon microreactor. Given the difference in thermal conductivities at these temperatures (roughly  $20 \text{ W m}^{-1}\text{K}^{-1}$  for silicon and  $0.10 \text{ W m}^{-1}\text{K}^{-1}$  for the gas mixture), such gradients are anticipated. Generally, Figures 7 and 8 show agreement: initial heat up, followed by cooling down.

## 4.2: Conclusions

All in all, given the simplifications necessary for convergence, this model is consistent with expected simulation profiles detailed by Blackwell. Mostly importantly, this model has succeeded in creating the necessary framework for simulating relevant chemical, thermal, and diffusional processes in a typical microreactor using propane combustion as a fuel source.

Though the implications of this simplified model are limited, several trends can be noted that are helpful for understanding the coupling of the overall system. For instance, the strongest dependencies of this model are those between the chemical and thermal modes. Species diffusion is related to the thermal profile of the geometry, but the chain of effect proceeds primarily in one direction: changes in temperature produce changes in diffusivity. In the case of the chemical and thermal coupling, the two processes are much more cyclical. Changes in temperature produce

changes in reaction rates, which in turn produce changes in the heat of reaction, which in turn produces changes in temperature.

Similarly, variations in thermodynamic properties play a much larger role in affecting this model than transport properties do. The strong dependence on temperature noted previously makes it important to have particularly accurate models for the chemical processes and thermal parameters. Since the transport properties are tied mostly to solving for the velocity field, their impact is not as great. Though the nonlinearity of this problem makes it difficult to form clear connections between parameters, these general relationships appear to hold true.

Unfortunately, many of the problems tackled in initially developing this first level model were focused on using the software itself. Because COMSOL has not yet gained a widespread user base, there does not exist much in the way of self-help guides. Sometimes just trying to figure out which module to apply in a certain situation is an issue in and of itself. Online support (in the way of forums and guides) is at an absolute minimum, and even the commercial COMSOL support does not always deliver results. Nonetheless, this model, though very complex, definitely takes advantage of COMSOL's fullest capabilities. Sitting down for a second round of work with this model would certainly see improved efficiency as the issues faced would be understanding physical problems (proper boundary conditions, couplings, etc), as opposed to figuring out how to use the software.

One issue faced by this work was a lack of overall possibility for validation. The only point of comparison was the work done by Blackwell, which provided a very high level view of the system. Though the assumptions regarding the chemical modeling seemed sound, validation at a lower level (perhaps for the fluid flow, chemistry, and heat transfer modules) would have given more confidence to the assumptions being made.

Overall, the experience of working on this thesis has definitely given me some more insight as to what life will be like as I enroll in a PhD program this spring. Perhaps the point I will take away most is the true interdisciplinary aspect of research. This project had thermal, fluid, and chemical elements are rolled up into one package, and therefore required me to do a lot of independent studying. I really enjoyed having the opportunity to challenge myself in this way, and look forward to what graduate school has to offer.

### 4.3: Future Work

The most important issue facing this model is in determining what issues prevented the ideal case from converging. First, it is necessary to check the underlying physics to make sure that the system is properly defined. Being able to validate individual physics applications as opposed to the entire model (as suggested in the previous section) would definitely help to accomplish this.

Another potential issue that warrants further investigation is in the numerical methods at play. In order to solve the various coupled differential equations, COMSOL takes the minimum amount of information from the user (material properties, boundary conditions, etc) and uses it to simulate the model. Virtually hidden from the user are calculations that COMSOL performs behind the scenes in order to determine gradients, fluxes, and other parameters necessary for computing a solution. It could be that hidden in these equations is an instance in which the automatic declaration of variables creates a division by zero or fails to preserve module coupling. Furthermore, issues regarding problems with the geometry itself could have also acted as barriers to convergence. All in all, these numerical problems are best targeted at COMSOL's support team. Given their refusal to support the current model in 3.5a, creating the same model in 4.2a could prove very beneficial. If nothing else, insight gained from working with the support team in the 4.2a environment could be applied retroactively to 3.5a.

Worth noting as well is the influence of the current geometry on the temperature distribution. Given the straight channel utilized by this model, the heat transfer effects of the serpentine pattern are not accounted for. This affects temperature distribution within the microreactor, which in turn directly affects reaction rates and diffusivities. While COMSOL does not feature the best environment for creating 3D geometries, it is possible to create these geometries in software such as Solidworks or AutoCAD and import them to the COMSOL environment. The only concern with this process is making sure that all of the surfaces are properly defined so that boundary conditions can be correctly imposed.

Aside from general tuning of the model to address the convergence issues, there are several other aspects that warrant further investigation. First, the role of thermal diffusion was completely dismissed in the original modeling of the system. Though literature [5] indicated that this was a fair assumption for the temperatures at play, some more concrete evidence would be desirable. Second, more in-depth analysis of the limits facing the microreactor would also

provide great insight to the system. In particular, the Thiele modulus determines whether the combustion reaction is kinetic or diffusion limited. This quantity is calculated as [11]:

$$\Phi_s = \frac{r_p^2(-r)}{D_{eff}C_s} \quad (26)$$

Here,  $r_p$  is the radius of the catalyst particle,  $r$  is the rate of the reaction,  $C_s$  is the surface concentration of the fuel, and  $D_{eff}$  is the effective diffusion coefficient in the catalyst. For S $\mu$ RE IV,  $r_p$  is equal to the thickness of the catalyst layer (50 $\mu$ m). As implied by the variable  $C_s$ , this parameter is suited to a model in which the reactions occur as surface reactions.

Finally, it was noted that in modeling the reaction rate, Blackwell used an equation similar to Equation 16 but with 1.1 as the exponent for propane and -0.5 as the exponent for oxygen. The effects of this alternative equation for reaction rate could also account for some of the differences observed in results.



## Appendix A: Parameter List

| Parameter  | Value   | Source |
|--|---|--------|
| Activation Energy ( $E_A$ ) for Propane                    | 89.1 kJ mol <sup>-1</sup>                               | [12]   |
| Frequency Factor (A)                                       | 7e5 (mol/m <sup>3</sup> ) <sup>-5</sup> s <sup>-1</sup> | *      |
| Transport Properties ( $\epsilon/k_B$ , $\mu$ , $\sigma$ ) | Various   | [13]   |
| Thermodynamic Fit Coefficients ( $c_p$ , $h$ , $s$ )       | Various   | [14]   |

\*NOTE: Inconclusive literature search led to choice of value evaluated through effect on simulation results.

# Bibliography

1. National Science Foundation Blue Ribbon Panel on Simulation-Based Engineering, S., *Revolutionizing engineering science through simulation : a report of the National Science Foundation Blue Ribbon Panel on Simulation-Based Engineering Science*. 2006, Arlington, VA: National Science Foundation.
2. Chan, Y. and A. National Meeting of. *Applications of microreactor in pharmaceutical development & production*. 2005.
3. Plazl, I., *Enzyme-catalyzed reactions at the microreactor scale : [invited lecture]*. New starting line for decision makers in bio-economy era, 2008.
4. Walker, C., E. Massachusetts Institute of Technology. Dept. of Electrical, and S. Computer, *Towards a high-efficiency micro-thermophotovoltaic generator*. 2010.
5. Blackwell, B.S. and E. Massachusetts Institute of Technology. Dept. of Chemical, *Design, fabrication, and characterization of a micro fuel processor*. 2008.
6. Curtiss, C.F. and R.B. Bird, *Multicomponent Diffusion*. INDUSTRIAL AND ENGINEERING CHEMISTRY RESEARCH, 1999. **38**(7): p. 2515-2522.
7. Bird, R.B., W.E. Stewart, and E.N. Lightfoot, *Transport Phenomena*. 1994, New York: John Wiley.
8. Gordon, S. and B.J. McBride, *Computer program for calculation of complex chemical equilibrium compositions, rocket performance, incident and reflected shocks, and Chapman-Jouguet detonations*. 1971, Washington: Scientific and Technical Information Office, National Aeronautics and Space Administration; [for sale by the National Technical Information Service, Springfield, Va.].
9. Reaction, D., *Getting started CHEMKIN Release 3.6.2*. 2001, San Diego, CA: Reaction Design.
10. Purdue University. Thermophysical Properties Research, C., P.E. Liley, and S.C. Saxena, *Thermophysical properties of matter... nonmetallic liquids and gases Vol.3, Thermal conductivity*. 1970.
11. Satterfield, C.N., *Heterogeneous catalysis in industrial practice*. 1991, New York: McGraw-Hill.
12. Wanke, S.E., *Oxidation of propane over a diesel exhaust catalyst*. Can. J. Chem. Eng. The Canadian Journal of Chemical Engineering, 1973. **51**(4): p. 454-458.
13. *Transport Properties of Various Chemical Species (CHEMKIN Format)*. [cited 2012 January 25]; Available from: <http://web.mit.edu/anish/www/transhrjhb1101.dat>.
14. *Thermodynamic Properties of Various Chemical Species (CHEMKIN Format)*. [Data Set] [cited 2012 January 25]; Available from: <http://web.mit.edu/anish/www/thermhrjhb1101.dat>.